Eddy Currents and Non-Conforming Sliding Interfaces for Motion in 3-D Finite Element Analysis of Electrical Machines

Stefan Böhmer, Christian Krüttgen, Björn Riemer, and Kay Hameyer

Institute of Electrical Machines, RWTH Aachen University, Aachen D-52062, Germany

This paper presents non-conforming sliding interfaces for motion in 3-D finite element simulations. Sliding interfaces are favorable, especially for field circuit coupling in comparison to other approaches such as the Lockstep method because an arbitrary position of the rotor is possible. A previously presented approach by the authors is extended to take eddy-currents into account. The sliding interfaces approach utilizes specific Lagrange multiplier to handle the relative motion between stator and rotor which require a magnetic scalar potential formulation. The formulation is presented as well as methods to compute the mandatory cohomology basis functions.

Index Terms— **Cohomology, eddy currents, electrical machines, sliding interfaces.**

I. Introduction

NUMERICAL simulation of electrical machines requires a flexible implementation of the rotor motion in 2-D and 3-D models. In contrast to the well-known approaches, such as Moving-Band or Lockstep method, sliding interfaces with non-conforming meshes between stator and rotor exhibit several advantages.

1) No remeshing is necessary between different time steps of a transient simulation.
2) Numerical errors attributable to the modified discretization are avoided.
3) Dynamic processes can be simulated with an arbitrary rotor position.

In particular, the last item is crucial for field circuit coupled finite element (FE) simulations. The continuity of the magnetic field across the non-conforming interface between the stationary and moving parts is ensured by the application of Lagrange multiplier. This yields a saddle point problem, which cannot be solved by standard iterative Krylov-subspace algorithms, such as the conjugate gradient algorithm. In order to preserve the numerical properties of a conforming approach, the FE-space of the discrete Lagrange multiplier is spanned by basis functions fulfilling the biorthogonality condition as described in [2] and applied to electromagnetic field computation in [3] and [4]. Thereby, the resulting system of equations is symmetric positive definite and can be solved by Krylov-subspace algorithms. In 2-D FE models, sliding interfaces can be applied to the magnetic vector potential formulation, whereas the required biorthogonal basis functions cannot be derived in a canonical way for 3-D FE magnetic vector potential formulations [3], but for magnetic scalar potential formulations.

Boehmer *et al.* [1] present a method to realize sliding interfaces by means of a magnetic scalar potential formulation for static FE simulations. For the operation of permanent magnet excited synchronous machines (PMSMs), especially with surface mounted permanent magnets eddy-current effects inside the magnets are not negligible. Eddy-current losses have to be considered particularly if rare earth permanent magnets with comparable high electrical conductivity are applied. In this paper, the static $\mathbf{t}$-ω formulation is extended to allow for the transient computation of magnetic fields including eddy-current effects in conducting regions.

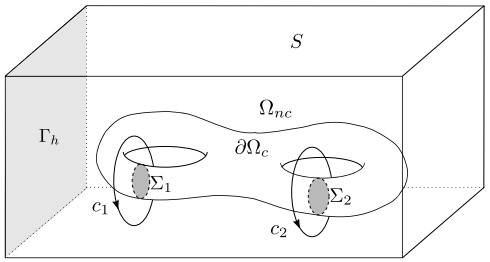

Fig. 1. Topological structure of the considered 3-D domain Ω, see [5].

This paper is organized as follows. After the short introduction and motivation in this section, the magnetic scalar potential formulation is described in detail in Section II. In Section III, two methods to compute the required cohomology basis functions are described and compared. Finally, a transient analysis of an exemplary PMSM is performed to present first numerical results of the applied method.

II. Formulation

Let Ω be a connected mesh, $\Omega_{\mathrm{nc}} \subset \Omega$ the non-conducting domain, $\Omega_c \subset \Omega$ the domain of all conductors, and $\partial\Omega_c$ its boundary, as shown in Fig. 1. In the following, we are going to employ the notation of differential forms to identify the electromagnetic fields. Let $W^p(\Omega)$ be the set of differential forms of degree p which are defined on the domain Ω. For example, the magnetic field $\mathbf{h}$ is a 1-form, which is integrated on curves. The flux density $\mathbf{b}$ and current density $\mathbf{j}$ are 2-forms and thus are integrated on surfaces. In the non-conducting domain, one has to solve $\operatorname{div} \mathbf{b} = 0$, $\operatorname{curl} \mathbf{h} = 0$,

Manuscript received June 5, 2014; revised August 25, 2014; accepted September 10, 2014. Date of current version April 22, 2015. Corresponding author: S. Böhmer (e-mail: stefan.boehmer@iem.rwth-aachen.de).

Color versions of one or more of the figures in this paper are available online at http://ieeexplore.ieee.org.

Digital Object Identifier 10.1109/TMAG.2014.2359155

and $\mathbf{b} = \mu_0 \mathbf{h}$ with $\mathbf{b} \in B(\Omega_{\rm nc})$ and $\mathbf{h} \in H(\Omega_{\rm nc})$

$$\begin{aligned} B(\Omega_{\rm nc}) &= \{\mathbf{b} \in W^2(\Omega_{\rm nc}),\ (\mathbf{b} - \mathbf{b}^0) \cdot \mathbf{n} = 0 \text{ on } \Gamma_b\} \\ H(\Omega_{\rm nc}) &= \{\mathbf{h} \in W^1(\Omega_{\rm nc}),\ \text{curl } \mathbf{h} \cdot \mathbf{n} = 0 \text{ on } \partial\Omega_{\rm nc} \\ &\qquad (h - h^0) \times \mathbf{n} = 0 \text{ on } \Gamma_h\}. \end{aligned} \tag{1}$$

While div $\mathbf{b} = 0$ can be satisfied by introduction of the magnetic vector potential $\mathbf{a}$ with $\mathbf{b} = \text{curl } \mathbf{a}$, the situation is more complicated for curl $\mathbf{h} = 0$. The Poincaré lemma states that $\mathbf{h}$ can be represented by a continuous gradient field ($\mathbf{h} = \text{grad } \omega$) in a contractible domain such as a sphere or a tetrahedron. If the domain contains holes and thus is not contractible, $\mathbf{h}$ cannot be represented by a gradient field anymore. But, let us first consider only simply connected non-conducting regions $\Omega_{\rm nc}$, which are contractible.

A. Simply Connected Non-Conducting Regions

In this case, the magnetic field $\mathbf{h} = \mathbf{t} - \text{grad } \omega$ is expressed by a single-valued magnetic scalar potential ω and an electric vector potential $\mathbf{t}$ with $\mathbf{j} = \text{curl } \mathbf{t}$ and $\mathbf{t} \in T(\Omega_c)$, $\omega \in W(\Omega)$ defined on

$$\begin{aligned} T(\Omega_c) &= \{\mathbf{t} \in W^1(\Omega_c),\ \text{curl } \mathbf{t} \cdot \mathbf{n} = 0 \text{ on } \partial\Omega_c\} \\ W(\Omega) &= \{\omega \in W^0(\Omega),\ \text{grad } \omega \times \mathbf{n} = 0 \text{ on } \Gamma_h\}. \end{aligned} \tag{2}$$

In regions without eddy currents, the static formulation can be applied

$$-\text{div } (\mu \text{grad } \omega) = -\text{div } \mathbf{b}_r - \text{div } \mu \mathbf{t}_0 \tag{3}$$

where μ is the permeability of the magnetic material. In eddy-current regions, the formulation of the electromagnetic field equations derived from the Maxwell equations is given by

$$\text{curl } \frac{1}{\sigma} \text{curl } \mathbf{t} + (\partial_t \mu \mathbf{t} - \partial_t \mu \text{grad } \omega) = 0 \tag{4}$$

$$\text{div } (\mu \mathbf{t} - \mu \text{grad } \omega) = -\text{div } \mathbf{b}_r \tag{5}$$

where σ is the specific electric conductivity. By using this formulation, it is possible to handle electromagnetic field problems on topological trivial domains. But, this limitation is not feasible in many cases, where the considered non-conducting domain contains holes.

B. Multiply Connected Non-Conducting Regions

Let us consider the two cycles c_1 and c_2 through the holes of the non-conducting region $\Omega_{\rm nc}$ around Ω_c, as shown in Fig. 1. If we evaluate the magnetic field $\mathbf{h}$ over the cycle c_1 or c_2, the result should equal the linked current in the conducting region to satisfy Ampère's law. In contradiction to this, the evaluation of the gradient of the magnetic scalar potential ω on the corresponding cycle must be zero

$$\int_{c_i} \mathbf{h} = I_i \neq 0 = \int_{c_i} \text{grad } \omega. \tag{6}$$

Thus, it is not possible to describe the magnetic field $\mathbf{h}$ in the non-conducting region only by the gradient of a scalar potential. One possible solution to solve this issue is to explicitly define cut surfaces which make the considered non-conducting domain simply connected and allow a jump of the magnetic scalar potential ω across the cut [6]. Defining such cut surfaces is troublesome if the examined geometry is complicated. The underlying homotopy-based definition of cuts can cause problems not only, if a knot's complement is present [7], but also if simple geometries are considered [8]. Another solution consists of considering the topological structure of the non-conducting domain, namely homology and cohomology [5], [8], [9]. Let $B^1(\Omega_{\rm nc})$ be the set of all gradients and $Z^1(\Omega_{\rm nc})$ the set of all curl-free fields on $\Omega_{\rm nc}$. Following De Rham's theorem, the quotient vector space

$$H^1(\Omega_{\rm nc}) = \frac{Z^1(\Omega_{\rm nc})}{B^1(\Omega_{\rm nc})} \tag{7}$$

is of finite dimension, which is equal to the number of holes in $\Omega_{\rm nc}$, respectively, the number of independent loops N_Σ formed by the conductors. This number plays an important role in topology and is also called Betti number β_1. For example, if the topological structure shown in Fig. 1 is examined, the Betti number β_1 of the non-conducting domain equals 2. Hence, the first cohomology group $H^1(\Omega_{\rm nc})$ represents the set of curl-free 1-forms which cannot be expressed by a gradient of a 0-form. These are exactly the forms we need to eliminate the contradiction in (6). Now, we can express the magnetic field $\mathbf{h}$ by

$$\mathbf{h} = \mathbf{t} - \text{grad } \omega + \sum_{k=0}^{\beta_1} I_k \mathbf{t}^k \tag{8}$$

where $\mathbf{t}^k \in H^1(\Omega_{\rm nc})$ are representatives of the first cohomology group $H^1(\Omega_{\rm nc})$ and the coefficients I_k are the linked currents corresponding to cycles in the first homology group $H_1(\Omega_{\rm nc})$. This group is defined as the set of all closed curves in $\Omega_{\rm nc}$ which are not the boundary of any surface in $\Omega_{\rm nc}$

$$H_1(\Omega_{\rm nc}) = \frac{Z_1(\Omega_{\rm nc})}{B_1(\Omega_{\rm nc})}. \tag{9}$$

The De Rham's theorem states that the first homology group is isomorphic to the first cohomology group $H_1(\Omega_{\rm nc}) \cong H^1(\Omega_{\rm nc})$. Thus, the two cycles $c_1, c_2 \in H_1(\Omega_{\rm nc})$ in Fig. 1 correspond to the linked currents I_1 and I_2 through the cross section surfaces Σ_1 and Σ_2 of the conducting region. The coefficients I_k may either be determined as excitation currents or are additional unknowns in eddy-current regions. If the second case applies, the system matrix is extended by a non-local equation regarding to the additional unknown.

In the following section, we are going to outline the different possibilities to compute the required cohomology basis functions.

III. Cohomology Computation

The connection between cuts for the magnetic scalar potential formulation and homology has been stated by Kotiuga almost 30 years ago [10]. Nevertheless, mainly heuristic approaches have been widely used to construct cuts for electromagnetic field problems due to the computational complexity of the homology and cohomology computation. By the straight forward approach, the cohomology groups can be computed by exploiting the Smith normal form (SNF) integer

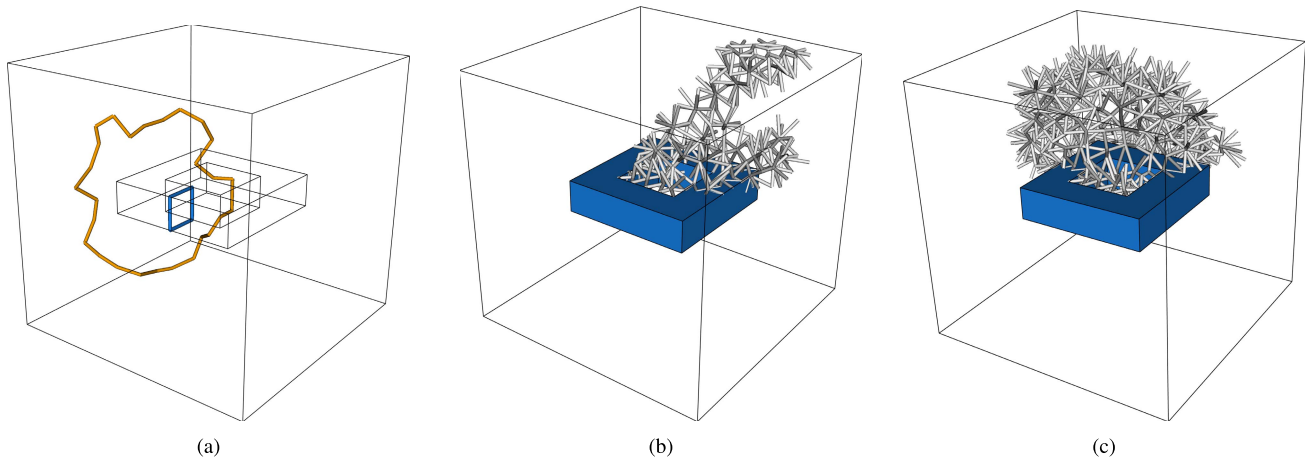

(a) (b) (c)

Fig. 2. Representatives of the first cohomology and homology group for example 3-D conducting torus (blue) contained in air. (a) Homology basis functions computed by Gmsh (orange) and constructed manually (blue). (b) Cohomology basis function, Gmsh. (c) Cohomology basis function, *i*MOOSE .

matrix decomposition. This algorithm exhibits a complexity of $O(n^3)$ with n being the number of edges in the considered domain. Therefore, it is not a feasible method to solve a electromagnetic field problem. In contrast to this, nowadays, there exist different approaches to compute cohomology groups in a reasonable time. In the following, we employ two different kinds of algorithms:

1) tree-cotree decomposition;
2) reduction techniques.

The first algorithm has been presented in [5] and generates a basis for the first cohomology group by the use of spanning trees. For this purpose, a basis for the first homology group $H_1(\Omega_{\mathrm{nc}})$ has to be given as input, which can be constructed manually in the modeling phase of the geometry. For example, representatives of $H_1(\Omega_{\mathrm{nc}})$ in Fig. 1 are obtained from the union of all edges of Σ_i and $\partial\Omega_{\mathrm{nc}}$. The termination of the algorithm depends strongly on the generated spanning tree, but also if the advantageous breadth first search is used to construct the tree, termination is not assured. Hence, Boehmer *et al.* [1] present a modification of the algorithm whose termination can be proofed.

Cohomology computation by reduction techniques consist of three steps:

1) create the chain complex corresponding to the FE mesh, which represents the topological structure of the domain;
2) homology invariant reduction of the chain complex [11];
3) SNF integer matrix decomposition.

The size of the chain complex after reduction is usually much smaller than the original complex, so that the high complexity of the SNF is no problem for the efficiency. Another approach utilizing so called lazy cohomology generators for application in electromagnetic field problems has recently been published [12].

In the following, both algorithms are applied to example geometry. The first one is implemented in the institute's in-house FE-package *i*MOOSE [www.iem.rwth-aachen.de] and a reduction technique algorithm [13] provided in Gmsh [14] is employed. The example geometry consists of a conducting torus contained entirely in air as shown in Fig. 2, which results in a Betti number $\beta_1 = 1$. The required

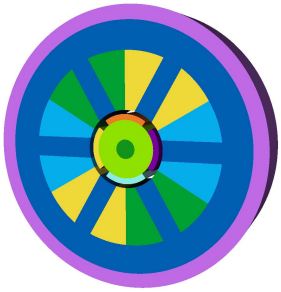

Fig. 3. Geometry of testcase PMSM.

representative of the first homology group $H_1(\Omega_{\mathrm{nc}})$ for *i*MOOSE has been created in beforehand and is visualized in blue color in Fig. 2(a) lying on the surface of the conducting torus $\partial\Omega_c$. The same figure shows the first homology group computed by Gmsh as highlighted orange edges. The support of the first cohomology basis constructed by *i*MOOSE and Gmsh can be observed from Fig. 2(b) and (c), respectively. The illustration indicates that the reduction algorithm exploited in Gmsh results in a much smaller support of edges of the cohomology basis function (#edges: 377) in comparison to the spanning tree algorithm in *i*MOOSE (#edges: 849). A smaller support is desired for the subsequent FE computation leading to fewer non-zero entries in the system matrix and hence to a better convergence of the iterative solution of the linear equation system. In addition, the time required for the cohomolgy computation in Gmsh is smaller when compared with *i*MOOSE, which may be due to the inefficient implementation in the scripting language Python in *i*MOOSE. Regarding these points, we are going to utilize the implementation in Gmsh for further applications.

IV. Numerical Results

The presented formulation has been implemented in the institute's in-house FE-package *i*MOOSE and is applied to a PMSM shown in Fig. 3. The considered machine has an active magnetic length of 120 mm and an outer stator radius of 65 mm. The rotor has four surface mounted permanent magnets, which have a height of 3 mm and are parallel magnetized with a remanence flux density of $\mathbf{b}_r = 1$ T.

TABLE I
FURTHER GEOMETRIC PARAMETERS

Parameter	Value
Width of the yoke	15 mm
Conductivity of the PM	$4.73 \cdot 10^5$ S/m^3
Airgap	2 mm
Pole covering	82.5 %
Rotor radius	15 mm
Tooth width	10.472 mm

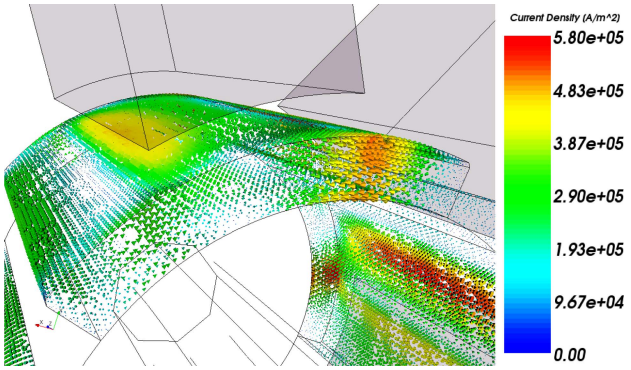

Fig. 4. Eddy currents in surface mounted magnets.

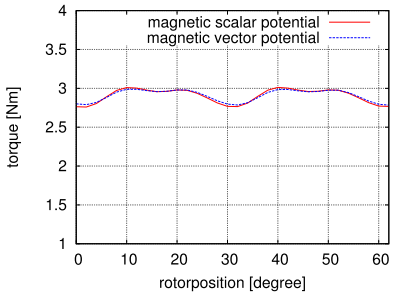

Fig. 5. Comparison of resulting torque with different approaches: magnetic vector potential and Lockstep method versus magnetic scalar potential and sliding interfaces.

The magnets are segmented into four parts in axial direction, each having a length of 30 mm, to avoid eddy currents along the entire axial length. So, it is sufficient to consider a model with the length of one segment. Further details of the geometric parameters can be found in Table I. The simulated operation point is selected to a speed of $n = 4000$ min^{-1} and a current of $I = 5$ A in each winding phase with 90 turns per coil. The 3-D geometry has been meshed in such a way, that it can be used for the Lockstep method, using a formulation with the magnetic vector potential as a reference simulation. The increment of the rotational displacement is fixed to $\Delta\alpha = 2°$. Nevertheless, the magnetic scalar potential approach was simulated with the sliding interface method. Application of the magnetic vector potential formulation results in ~3 million degrees of freedom, whereas the magnetic scalar potential formulation only requires 600 000 unknowns. Fig. 4 shows the resulting eddy-current distribution in the surface mounted permanent magnets. The resulting torque of the magnetic scalar and vector potential formulations has been calculated and scaled to the equivalent full length PMSM torque. These torques are compared in Fig. 5 and show a good agreement.

V. CONCLUSION

This paper presents a magnetic scalar potential formulation for the use with sliding interfaces to analyze eddy currents in rotating electrical machines. The advantages of the sliding interfaces method, especially the arbitrary rotor position for dynamic processes without remeshing, can now be utilized also in the field of eddy-current problems.

Furthermore, the advantage of the magnetic scalar potential formulation, which consists of a much lower number of degrees of freedom in contrast to magnetic vector potential formulations, resulting in smaller computational efforts is an additional benefit in 3-D FE analysis of electrical machines.

Future research will include the application on more complex problems and field circuit coupling to show the advantage of the arbitrary rotor position in contrast to the Lockstep method.

REFERENCES

[1] S. Boehmer, E. Lange, and K. Hameyer, "Non-conforming sliding interfaces for relative motion in 3D finite element analysis of electrical machines by magnetic scalar potential formulation without cuts," *IEEE Trans. Magn.*, vol. 49, no. 5, pp. 1833–1836, May 2013.

[2] B. Wohlmuth, "A comparison of dual lagrange multiplier spaces for mortar finite element discretizations," *ESAIM, Math. Model. Numer. Anal.*, vol. 36, no. 6, pp. 995–1012, Nov. 2002.

[3] E. Lange, F. Henrotte, and K. Hameyer, "Biorthogonal shape functions for nonconforming sliding interfaces in 3-D electrical machine FE models with motion," *IEEE Trans. Magn.*, vol. 48, no. 2, pp. 855–858, Jan. 2012.

[4] E. Lange, F. Henrotte, and K. Hameyer, "A variational formulation for nonconforming sliding interfaces in finite element analysis of electric machines," *IEEE Trans. Magn.*, vol. 46, no. 8, pp. 2755–2758, Aug. 2010.

[5] F. Henrotte and K. Hameyer, "An algorithm to construct the discrete cohomology basis functions required for magnetic scalar potential formulations without cuts," *IEEE Trans. Magn.*, vol. 39, no. 3, pp. 1167–1170, May 2003.

[6] Z. Ren, "T-Ω formulation for eddy-current problems in multiply connected regions," *IEEE Trans. Magn.*, vol. 38, no. 2, pp. 557–560, Mar. 2002.

[7] A. Bossavit, *Computational Electromagnetism: Variational Formulations, Complementarity, Edge Elements*. New York, NY, USA: Academic, 1998.

[8] P. Dlotko and R. Specogna, "Cohomology in 3D magneto-quasistatics modeling," *Commun. Comput. Phys.*, vol. 14, no. 1, pp. 48–76, Jan. 2013.

[9] M. Pellikka, S. Suuriniemi, L. Kettunen, and C. Geuzaine, "Homology and cohomology computation in finite element modeling," *SIAM J. Sci. Comput.*, vol. 35, no. 5, pp. B1195–B1214, 2013.

[10] P. R. Kotiuga, "On making cuts for magnetic scalar potentials in multiply connected regions," *J. Appl. Phys.*, vol. 61, no. 8, pp. 3916–3918, 1987.

[11] T. Kaczyski, M. Mrozek, and M. Lusarek, "Homology computation by reduction of chain complexes," *Comput. Math. Appl.*, vol. 35, no. 4, pp. 59–70, Feb. 1998.

[12] P. Dlotko and R. Specogna, "Lazy cohomology generators: A breakthrough in (Co)homology computations for CEM," *IEEE Trans. Magn.*, vol. 50, no. 2, Feb. 2014, Art. ID 7014204.

[13] M. Pellikka, S. Suuriniemi, and L. Kettunen, "Powerful heuristics and basis selection bring computational homology to engineers," *IEEE Trans. Magn.*, vol. 47, no. 5, pp. 1226–1229, May 2011.

[14] C. Geuzaine and J.-F. Remacle, "Gmsh: A 3-D finite element mesh generator with built-in pre- and post-processing facilities," *Int. J. Numer. Methods Eng.*, vol. 79, no. 11, pp. 1309–1331, Sep. 2009.